Dynamics of Combined Solitary-waves in the General Shallow Water Wave Models

Woo-Pyo Hong

Department of Physics, Catholic University of Daegu, Hayang, Kyongsan, Kyungbuk 712-702, South Korea and Department of Physics, University of British Columbia 6224 Agricultural Road, Vancouver, B. C. Canada V6T 1Z1

Reprint requests to Prof. W.-P. H. E-mail: wphong@mail.cu.ac.kr

We find new analytic solitary-wave solutions, having a nonzero background at infinity, of the general fifth-order shallow water wave models using the hyperbolic function ansatz method. We study the dynamical properties of the solutions in the combined form of a bright and a dark solitary-wave by using numerical simulations. It is shown that the solitary-waves can be stable or marginally stable, depending on the coefficients of the model. We study the interaction dynamics by using the combined solitary-waves as the initial profiles to show the formation of sech^2-type solitary-waves in the presence of a strong nonlinear dispersion term. – PACS: 03.40.Kf, 02.30.Jr, 47.20.Ky, 52.35.Mw

Key words: Fifth-order Shallow Water Wave Models; Analytic Combined Solitary-wave Solution; Numerical Simulation; Stability; Interaction.

1. Introduction

While it is easy to write down in closed form a solitary wave solution for the simplest standard model, namely the Korteweg-de Vries (KdV) equation, it has proved quite difficult to obtain the existence of such solutions for the problems from which the KdV equation was derived as a first approximation [1]. As such KdV hierarchy models, we investigate generalized fifth-order shallow water-wave equations which describe certain physically-interesting (1+1)-dimensional waves [1] (see Kichenassamy and Olver [2] regarding physics motivations for this type of models):

$$v_t + \alpha v_{xxxxx} + \mu v_{xxx} + \gamma \partial_x [2vv_{xx} + v_x^2]$$
$$+ 2qvv_x + 3rv^2 v_x = 0, \tag{1}$$

where α, μ, γ, q, r are model parameters, $v(x,t)$ is a real scalar function and the subscripts denote partial derivatives. The equation reduces to the standard KdV equation for $\mu = 1$ and $q = 3$ or $\mu = 1$ and $q = 1$, depending on the normalization scheme, with $\alpha = \gamma = r = 0$. Equation (1) also contains some higher-order approximations to the (third-order) KdV equation, and in fact it can be reduced to the fifth-order KdV equation only for $q\gamma = 3r\mu$ and $3\gamma\mu = 5q\alpha$, in which case there is a family of exact sech^2-type solutions [2].

The equation has been previously investigated by many authors due to its richness in mathematical and physical properties [1 – 8]. It has been shown by Benjamin et. al. [3] and Weinstein [4] that solitary-wave solutions exist in the case of $\gamma = 0$ and $\mu < 0$. Meanwhile Amick and Toland [5] have proven the existence of solitary-waves of speed -1, if $\alpha = 1$, $r = \gamma = 0$, $q = 1$, and μ is less than some positive number. Kichenassamy also has shown that there exist nontrivial solitary-waves if $\alpha > 0, r \le 0, q \ne 0$, and $\mu > 0$, without presenting explicit analytic solitary wave solutions [1]. More recently, some new analytic solitary-wave solutions have been found by the authors in [6 – 8] by using the tanh-method [9] or applying the truncated Painlevé expansion [10 – 12].

In this paper, we show that (1) bears new solitary-wave solutions with two peaks, i.e. a combined state of a dark and a bright solitary-wave, and investigate their dynamics by numerical simulations. In Sect. 2 we introduce an ansatz which allows to show the existence of a combined solitary-wave solution and to perform a symbolic computation to find the necessary constraints for such solutions. In Sect. 3 we numerically investigate the stability of the combined solitary-waves by utilizing the Fourier Spectral method [13]. In particular, we study the interaction dynamics by using the two solitary-waves as initial profiles in the presence of

strong nonlinear dispersion coefficients. Our conclusions follow in Section 4.

2. Analytic Solitary-wave Solutions

In this section, we would like to apply a generalized hyperbolic function method similar to those in [14–16] as an ansatz to find a solution of (1) in the form

$$v(x,t) = \sum_{m=0}^{M} A_m(t)\text{sech}^m[G(t)x + H(t)] \qquad (2)$$

$$+ \sum_{n=0}^{N} B_n(t)\text{sech}[G(t)x + H(t)]\tanh^n[G(t)x + H(t)],$$

where N and M are integers determined via the balance of the highest-order contributions from both the linear and nonlinear terms of (1), while $A_m(t)$, $B_n(t)$, $G(t)$, and $H(t)$ are differentiable functions which are related to the wave amplitude. Note that our ansatz is different from those is [14–16] by the fact that $\tanh^m\psi$ is replaced by $\text{sech}^m\psi$. An advantage for adopting such an ansatz is obviously the possibility of finding more interesting solutions beyond the usual bright and dark solitary-waves represented by only the powers of $\text{sech}\psi$ or $\tanh\psi$. The main purpose of this section is to show that the combined dark and bright solitary-wave solutions indeed exist under certain constraints satisfied by the model coefficients.

With the ansatz (2) we can determine M and N from various physical constraints between the model coefficients such as dispersion, dissipation, and nonlinearity, either separately or in various combinations. In our case, the highest order dispersion term v_{xxxxx} has $\text{sech}^{M+5}\psi$ and $\text{sech}\psi \cdot \tanh^{N+5}\psi$, and the highest nonlinear dispersion term v^2v_x has $\text{sech}^{3M+1}\psi$ and $\text{sech}\psi \cdot \tanh^{3N+3}\psi$, from which we get

$$M = 2 \text{ and } N = 1. \qquad (3)$$

In the following, we adopt a traveling solitary-wave ansatz with constraint amplitude in the form

$$v(x,t) = \sum_{m=0}^{N=2} A_m \cdot \text{sech}^m(kx + \omega t) \qquad (4)$$

$$+ \sum_{n=0}^{M=1} B_n \cdot \text{sech}^n(kx + \omega t) \cdot \tanh^n(kx + \omega t),$$

where the parameters A_m, B_n, ω, and k can all be complex. However, for the simplicity, *they are all taken*

to be real, as for this case only physically meaningful solitary-wave solutions may be obtained. On substituting the ansatz (4) into (1), equating to zero the coefficients of like powers of $\tanh\psi$, we obtain 13 very complicated equations to be solved simultaneously to find A_m, B_n, k, ω, and the necessary constraints among the model coefficients. However, because it is impossible to handle the equations even using symbolic packages like *Maple* or *Mathematica*, we put a special constraint on the amplitudes, i. e.

$$A_1 + B_0 = 0, \qquad (5)$$

since $A_1 + B_0$ is the common factor for the 6 equations. This constraint in fact is equivalent to eliminate the first order sech-term from (4). Under this constraint, we have the following 7 equations to solve:

$$3A_0^2kr + (2qk + 2\gamma k^3)A_0 + \omega + k^5\alpha + k^3\mu = 0, \quad (6)$$

$$6A_0^2kr + (-18rA_2k + 4qk + 40\gamma k^3)A_0 - (6qk + 42\gamma k^3)A_2$$
$$- 3krB_1^2 + 20k^3\mu + 182k^5\alpha + 2\omega = 0, \qquad (7)$$

$$9rB_1^2 - 15rA_2^2 + (216k^2\gamma + 8q + 24rA_0)A_2$$
$$- 840\alpha k^4 - 24\mu k^2 - 48k^2\gamma A_0 = 0, \qquad (8)$$

$$3rA_2^2 - rB_1^2 - 32k^2\gamma A_2 + 120\alpha k^4 = 0, \qquad (9)$$

$$6rA_2kA_0^2 + (-6krB_1^2 - 4qA_2k - 16\gamma k^3A_2)A_0 \qquad (10)$$
$$+ (-6\gamma k^3 - 2qk)B_1^2 - 8\mu A_2k^3 - 2A_2\omega - 32\alpha A_2k^5 = 0,$$

$$(120\alpha k^4 + 12k^2\gamma A_0 + 6\mu k^2 - 3rB_1^2)A_2 \qquad (11)$$
$$- (q + 12k^2\gamma + 3rA_0)A_2^2 + (3rA_0 + 18k^2\gamma + q)B_1^2 = 0,$$

$$-rA_2^3 + 16k^2\gamma A_2^2 + (-120\alpha k^4 + 3rB_1^2)A_2 \qquad (12)$$
$$- 16k^2\gamma B_1^2 = 0.$$

In order to further reduce the remaining equations, we assume an additional constraint on the amplitudes, i. e.

$$A_0 + A_2 = 0, \qquad (13)$$

which is equivalent to replacing the first part of (4) by $\tanh^2(kx + \omega t)$. This constraint results in the solitary-wave to have the same value at both infinities. Note that the $A_0 + A_2 = \boldsymbol{B} \neq 0$ constraint would only yield an additional constant term. Under these constraints on the amplitudes, from (9), we find

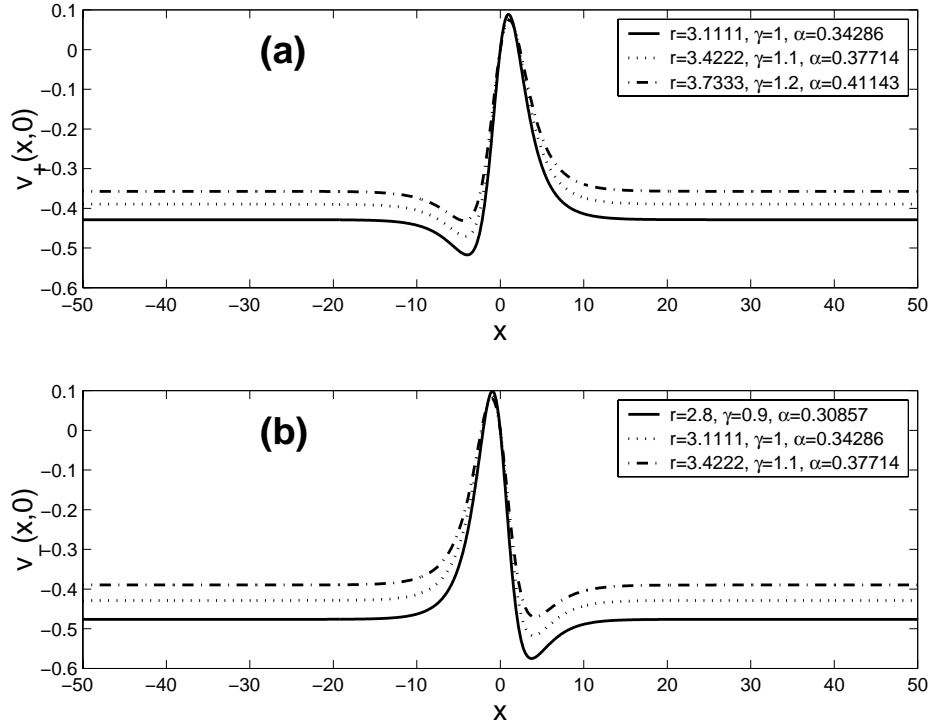$$B_1^2 = \frac{120\alpha k^4 - A_2(32\gamma k^2 - 3rA_2)}{r}. \qquad (14)$$

Fig. 1. (a) $v_+(x,0)$ with positive B_1 and (b) $v_-(x,0)$ with negative B_1 amplitude, respectively, for three different values of r satisfying $r > 20\gamma/9$, γ, and α. The combined solitary-waves (CSWs) have minimum and maximum peaks with a nonzero background value, i.e., $-A_2$ as $|x| \to \infty$.

This condition leads to the simplification of (12)

$$(8k^2\gamma A_2 - 30\alpha k^4 - rA_2^2)(-rA_2 + 8\gamma k^2) = 0, \quad (15)$$

which result in three possible solutions for the amplitude $A_2 = -A_0$, namely

$$A_2 = 8\frac{\gamma k^2}{r}, \quad A_2 = \frac{(8\gamma \pm 2\sqrt{16\gamma^2 - 30r\alpha})k^2}{2r}. \quad (16)$$

In the rest of the paper, we consider only the first amplitude, i.e., $A_2 = -A_0 = 8\frac{\gamma k^2}{r}$, since the others will yield similar solitary-waves, under different constraints among the model coefficients. After substituting (16) into the above remained equations, one finds the fifth-order dispersion relation for $\omega(k)$ from (10) as

$$\omega(k) = \frac{k^3(16q\gamma - 176\gamma^2 k^2 - \alpha k^2 r - \mu r)}{r}, \quad (17)$$

where $\omega(k)$ is defined as the angular frequency and k is the wave number. Subsequently, we obtain the wave number from (7) as

$$k^2 = \frac{1}{30}\frac{8q\gamma - 3\mu r}{4\gamma^2 - r\alpha}. \quad (18)$$

Under these conditions on the amplitudes and the given $\omega(k)$ and k, the initial 13 equations reduce to the following final constraint to be satisfied among the model coefficients

$$-9\mu\gamma r + 4q\gamma^2 + 5qr\alpha = 0, \quad (19)$$

which comes from (11). We note that there are two fixed coefficients in (1), i.e. $\mu = 1$ and $q = 3$ or $\mu = 1$ and $q = 1$, depending on the normalization scheme of (1). In the rest of the paper, however, we adopt $\mu = 1$ and $q = 3$ to find

$$\alpha = \frac{\gamma(3r - 4 - \gamma)}{5r}, \quad (20)$$

which shows that the highest dispersion term is balanced with the various nonlinear terms in (1). To sum
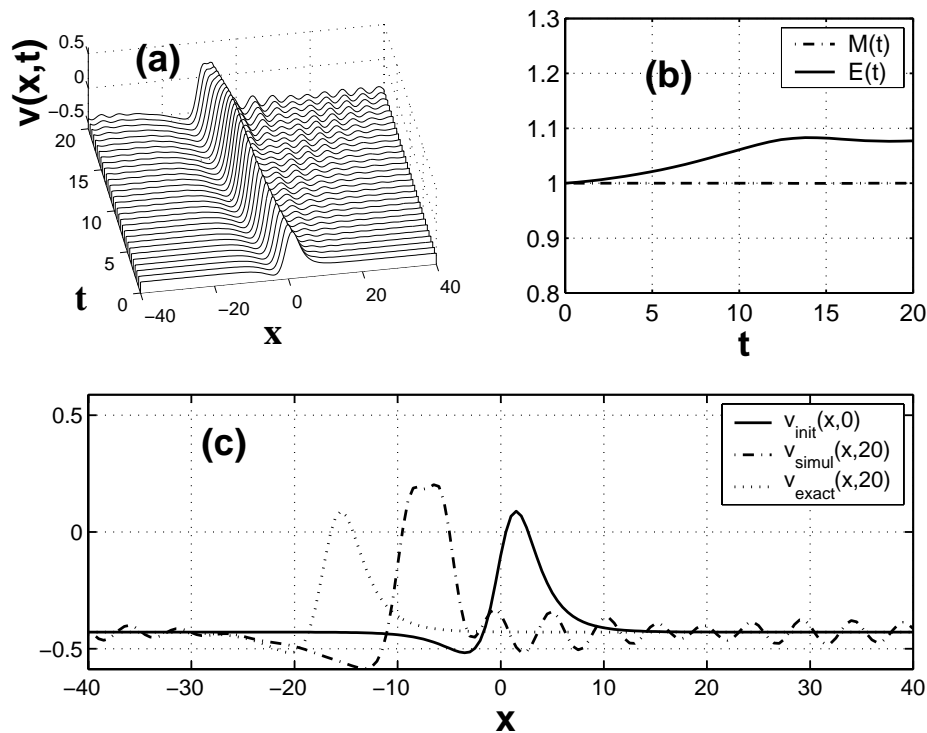
Fig. 2. (a) Evolution of the initial CSW with a positive B_1 amplitude and with $\gamma = 1$, $\alpha = 0.34286$, and $r = 3.1111$. (b) Variations of the normalized mass $M(t)$ and energy $E(t)$. $M(t)$ conserves its initial value, however $E(t)$ slowly increases before saturating to a constant value after $t = 12$. (c) Comparison of the numerically simulated profile at $t = 20$ with that of the exact CSW from (21), showing that the CSW becomes unstable by emitting radiation in the form of an oscillating tail.

up, a new analytic solitary-wave solution of (1) has been obtained as

$$v(x,t) = -A_2 \tanh^2(kx + \omega t)$$
$$+ B_1 \operatorname{sech}(kx + \omega t) \tanh(kx + \omega t), \quad (21)$$

where

$$k = \pm \frac{1}{\sqrt{6\gamma}}, \ A_2 = \frac{4}{3r}, \ ; B_1 = \pm \sqrt{\frac{2(20\gamma - 9r)}{9\gamma r^2}},$$

$$\omega = \pm \frac{\sqrt{6}(188\gamma - 11r)}{360\gamma^{3/2}r}, \quad (22)$$

with the constraint (20) among the coefficients. Thus, we can determine the allowed coefficient region for (r, γ), by requiring k and B_1 to be real, as

$$\gamma > 0 \ \text{and} \ r > \frac{20\gamma}{9}. \quad (23)$$

We find, as usual, the group speed $v_g = \partial\omega/\partial k$ and the phase speed $v_p = \omega/k$ of the dark-bright solitary-wave as

$$v_g = \frac{7r + 4\gamma}{12\gamma r}, \quad v_p = \frac{188\gamma - 11r}{60\gamma r}. \quad (24)$$

As shown in Figs. 1(a) and 1(b), for $v_+(x,0)$ with positive B_1 and $v_-(x,0)$ with negative B_1 for three different values of r, γ, and α, the solitary-wave does portray some interesting properties: First, it has both a minimum and a maximum peak due to the antisymmetric function $B_1 \operatorname{sech}(kx) \tanh(kx)$ and the symmetric function $A_2 \tanh(kx)^2$. Second, it has a non-vanishing background at infinity, i.e., $\lim_{x \to \pm\infty} v(x,t) = -A_2$, which depends only on the highest nonlinear dispersion coefficient r. In the rest of paper we denote the combined solitary-wave as CSW and study its dynamical properties by numerical simulations.
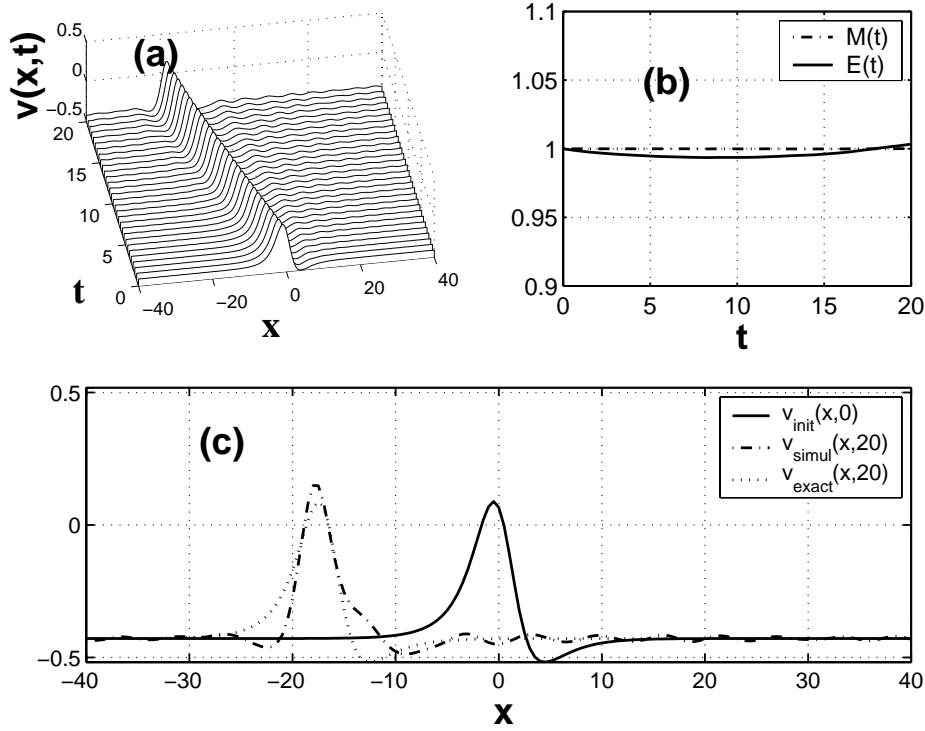
Fig. 3. The same coefficients as in Fig. 2 but with the negative B_1 amplitude. (a) Evolution of the initial CSW. The CSW emits less radiation than in Fig. 2(a). (b) The total energy $E(t)$ is shown to be approximately conserved because of the reduced radiation in comparison with that in Figure 2(a). (c) Comparison of the numerically simulated profile at $t = 20$ with that of the exact CSW from (21). Note that the core part of the CSW separates from the rest of the oscillating tail and resembles to the shape of a sech^2-type solitary-wave as it further evolves.

3. Dynamics of the Combined Solitary-waves

In this section we numerically integrate (1) to understand the stability and dynamics of the CSWs discussed in section 2. Here, the definition of "stability" means that the analytic solitary-wave preserves, when it is substituted to (1) and numerically integrated, its initial profile for a long propagation time without losing the total energy by radiation. The numerical scheme used in this work is based on the Runge-Kutta fourth-order scheme for the time domain and pseudo-spectral method using the discrete fast Fourier transformation in the spatial discretization [13], applying periodic boundary conditions. The numerical errors in the spatial discretization were controlled by varying the number of discrete Fourier modes between 128 and 1024. Various time steps between 10^{-5} and 10^{-3} are chosen for a stable wave propagation.

For the following analysis, we take the CSWs from (21) as initial profiles in the form

$$v_\pm(x) = -\sqrt{\frac{2(20\gamma - 9r)}{9\gamma r^2}} \tag{25}$$

$$\cdot \left[\tanh^2(\frac{x}{\sqrt{6\gamma}}) \pm \mathrm{sech}(\frac{x}{\sqrt{6\gamma}}) \tanh(\frac{x}{\sqrt{6\gamma}}) \right],$$

by setting $B_2 = A_1$, for convenience, which is satisfied under $r = 28\gamma/9$. Before proceeding, we note that (1) is in general non-integrable equation, it is not certain whether the equation contains infinite numbers of time-independent integrals. However, as at least the fundamental CSWs indeed do exist, we want to define the simplest two such integrals, namely the normalized
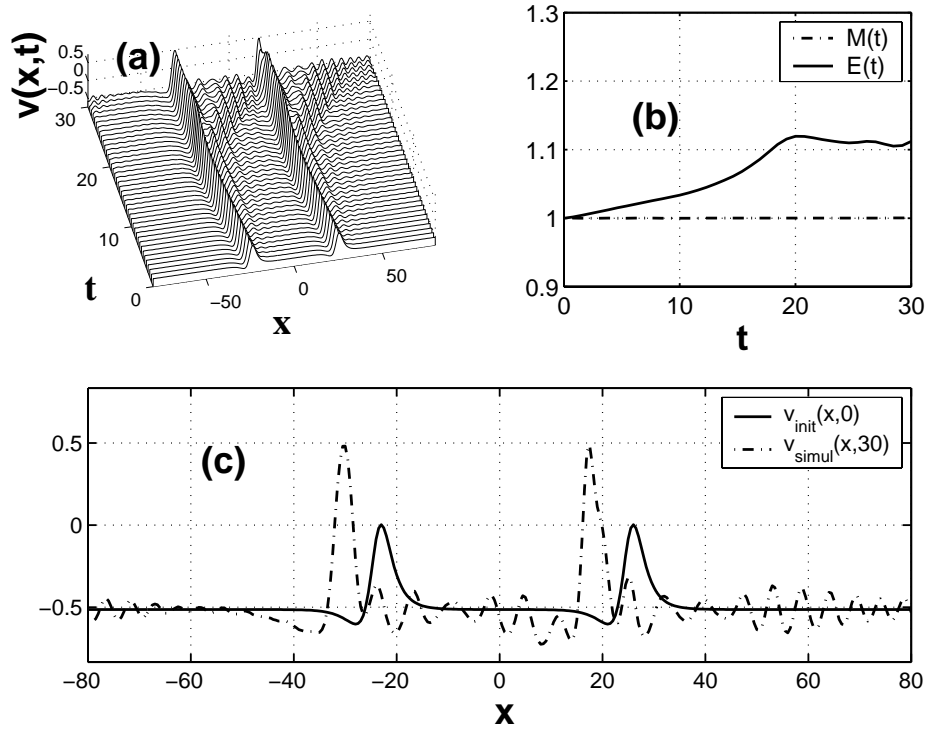
Fig. 4. (a) Interaction dynamics of two CSWs with the initial profile $v_+(x+\delta)+v_+(x-\delta)$, where $\delta = 10$, with the same coefficients as in Figure 3. The CSWs start interacting as soon as the radiation in the form of an oscillating tail is emitted. (b) The interaction process is considerably inelastic in the sense that $E(t)$ increases by more than 10%. (c) Snapshot of CSWs at $t = 30$ (dot-dashed curve), showing a strongly oscillating tail.

mass and energy

$$M(t) = \int_{-\infty}^{\infty} v(x,t)\mathrm{d}x / \int_{-\infty}^{\infty} v(x,0)\mathrm{d}x,$$
$$E(t) = \int_{-\infty}^{\infty} v(x,t)^2\mathrm{d}x / \int_{-\infty}^{\infty} v(x,0)^2\mathrm{d}x, \qquad (26)$$

respectively, to further understand the dynamics of the solitary-waves. Fig. 2(a) shows the evolution of CSW for the coefficients belonging to Fig. 1(a), namely $\gamma = 1$, $\alpha = 0.34286$, and $r = 3.1111$. In Fig. 2(c), we compare the numerically simulated profile at $t = 20$ with that of the exact CSW from (21), showing that the simulated CSW becomes unstable by emitting radiation in form of the oscillating tail. This radiation process acts as an effective friction, so that the speed of the solitary-wave gradually decreases along its propagation. Meanwhile, from Fig. 2(b) we find that the mass integral $M(t)$ conserves the initial value, but $E(t)$ slowly increases before saturating to a constant value after $t = 12$, which is due to the fact that the core of the

CSW is isolated from the radiation. By using the same set of coefficients as in Fig. 2, we simulate the propagation of the CSW with the negative B_1 amplitude in Figure 3. In comparison to Fig. 2 with a positive B_1 amplitude, the CSW in this case emits less radiation during the propagation as depicted in Figure 3(b). As the result, the phase speed of the CSW core is close to that of the exact solution (dot-dashed curve) at $t = 20$ in Figure 3(c). However, it should be noted that the core part of the CSW separates from the rest of the oscillating tail and resembles to the shape of a sech^2 solitary-wave as it further evolves.

Even though the CSWs considered above are unstable, it is still interesting to know their interaction dynamics. Thus, we consider the evolution of two CSWs with the following initial profiles:

$$v(x,0)_{\mathrm{init}} = v_\pm(x+\delta,0)+v_\pm(x-\delta,0), \qquad (27)$$

where δ is the separation between the solitary-waves. By using the same set of coefficients as in Figs. 2–3,
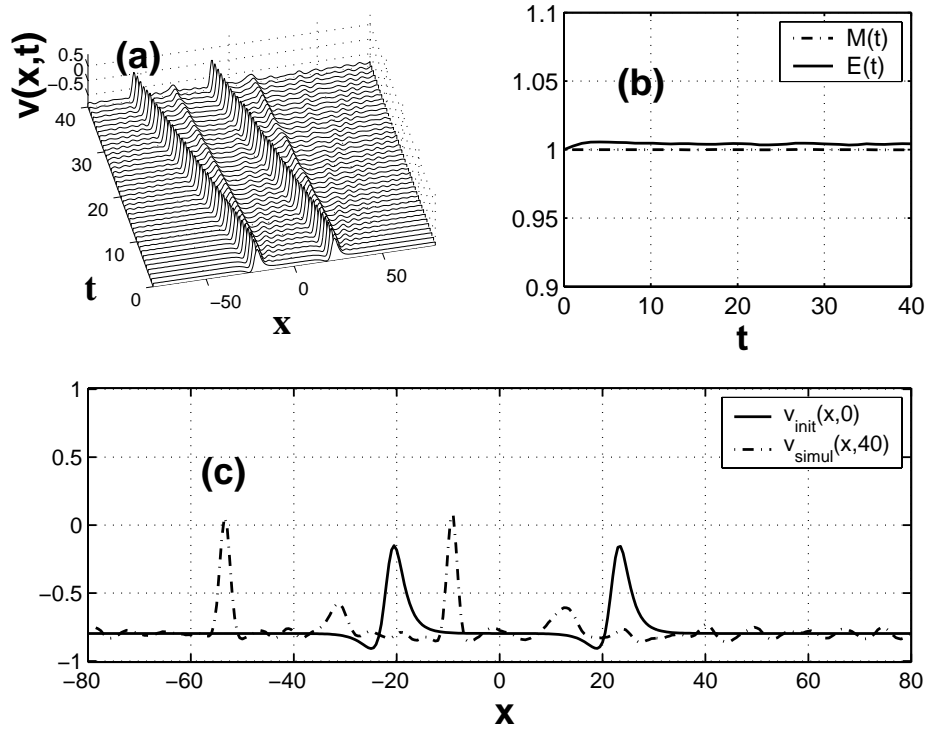
Fig. 5. The same initial profile as in Fig. 4 but with $\gamma = 0.8$, $\alpha = 0.274$, and $r = 2.488$. (a) A more stable interaction is shown. (b) $E(t)$ almost conserves the initial value, indicating a smaller amount of emitted radiation. (c) Snapshot of CSWs at $t = 30$.

the interaction dynamics of the CSWs with $v_+(x+\delta) + v_+(x-\delta)$, separated by $\delta = 10$, is shown in Figure 4. Initially, the CSWs do not influence each other, but they start interacting as soon as the radiation in the form of an oscillating tail is emitted, as shown in Figure 4(a). From Fig. 4(b) we observe that the whole interaction process is 'inelastic' in the sense that $E(t)$ increases by more than 10% from the initial value and saturates to a constant value for $t > 20$, owing to the presence of the oscillating tail. Fig. 4(c) presents the snapshot of $v(x,t)$ at $t = 30$ (dot-dashed curve), showing a strongly oscillating tail. By choosing a different set of coefficients, for example $\gamma = 0.8$, $\alpha = 0.274$ and $r = 2.488$, which leads to a higher amplitude than that in Fig. 4, we demonstrate that the CSW core takes the shape of a sech^2-type solitary-wave when the emitted radiation interacts with the lower peaks of the CSWs as shown in Figs. 5(a) and 5(c). We also note that the normalized energy in Fig. 5(b) varies by less than 1% during the interaction and in fact saturates to a constant value. After many simulations, we conclude that some

variation in $E(t)$ is a general tendency since the nonlinear dispersion coefficient r decreases with decreasing γ value, however with increasing amplitude. It is worth mentioning that, as δ decreases the evolution time at which the core separates from the rest of radiation is also shortened.

Finally, we investigate in Fig. 6 the evolution of CSWs with the reversed polarity, i.e. with the initial profile as $v_-(x+\delta) + v_-(x-\delta)$, making the choice $\gamma = 0.7$, $\alpha = 0.24$, and $r = 2.178$. In comparison with Figs. 5(a) and 5(b), the formation of a sech^2-type solitary-wave in the core is shown to be more evident in Figs. 6(a) and 6(b), indicating an elastic process in the sense that $E(t)$ is almost constant during the interaction process. This can be understood by comparing $v_+(x,t)$ in Fig. 2 with $v_-(x,t)$ in Fig. 3, where the minimum peak of the former is located at the leading side while for the latter it is located at the trailing side. Therefore, a more stable sech^2-type solitary-wave in the core is formed under less oscillating radiation background.
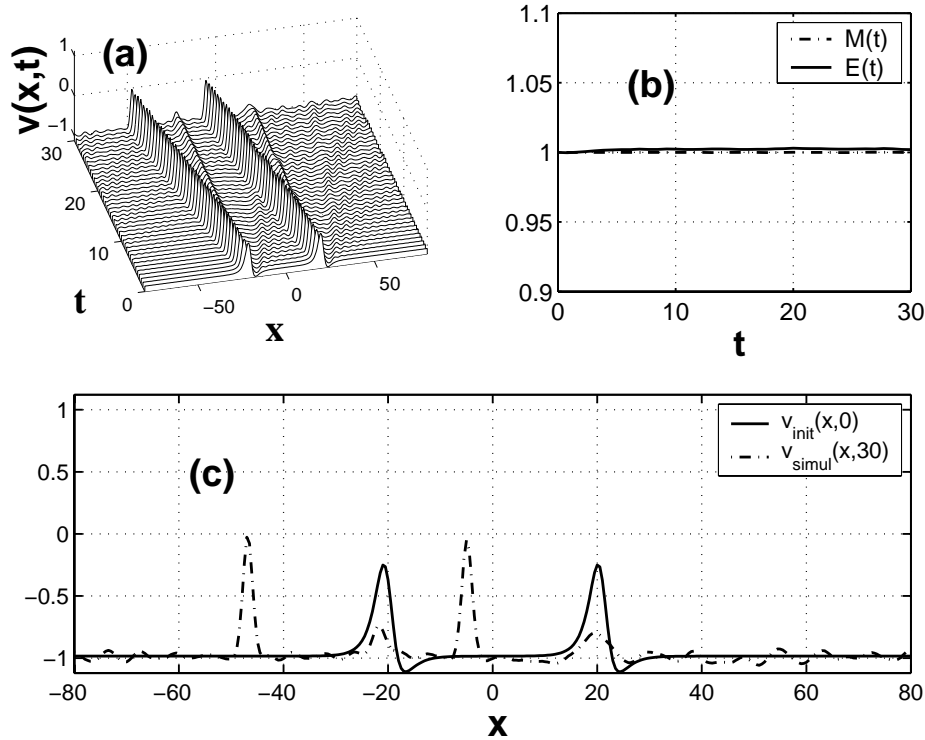
Fig. 6. (a) Interaction dynamics of two CSWs with the initial profile $v_-(x+\delta) + v_-(x-\delta)$ where $\delta = 10$, with the same coefficients $\gamma = 0.7$, $\alpha = 0.24$, and $r = 2.178$. (b) $E(t)$ is almost constant during the interaction process, which indicates that the interaction is close to an elastic one. (c) Snapshot of CSWs at $t = 30$ (dot-dashed curve), showing the formation of a sech²-type solitary-wave in the core.

4. Conclusions

In this work, we have found a new analytic coupled solitary-wave solution, having a nonzero background at infinity, of the general fifth-order shallow water-wave model using the hyperbolic function ansatz method similar to [14–16]. The CSW solution in (21)–(22) exists under the balance condition (20) in the coefficient region in (23). Even though it has not been analyzed here, two additional families of solutions do exist for the different amplitudes as shown in (16). We have shown by numerical simulations that the CSWs are unstable and emit radiation in the form of an oscillating tail during their propagation, as depicted in Figs. 2 and 3. It is noted that the high resolution numerical scheme adopted in this work guarantees that the radiation is not a numerical noise but the dynamical nature of the CSW. The interaction dynamics of two CSWs has been investigated in

Figs. 4–6 for the cases of the same initial polarities, i.e. the same B_1 amplitudes. By examining $M(t)$ and $E(t)$ as defined in (26), we can conclude that the interaction process is not exactly elastic. However, depending on the coefficients and polarities of the two CSWs, in particular, an almost elastic interaction has been shown to occur in Fig. 6. The fact that the cores of the CSWs during the interaction resembles sech²-type solitary-waves has been cleary demonstrated in Figures 5 and 6.

[1] S. Kichenassamy, Nonlinearity **10**, 133 (1997).

[2] S. Kichenassamy and P. J. Olver, SIAM J. Math. Anal. **23**, 1141 (1992).

[3] T. B. Benjamin, J. L. Bona, and D. K. Bose, Phil. Trans. Roy. Soc. **A331**, 195 (1990).

[4] M. Weinstein, Commun. PDE **12**, 1133 (1987).

[5] C. J. Amick and J. F. Toland, Euro. J. Appl. Math. **3**, 97 (1992).

[6] W. P. Hong and Y. D. Jung, Z. Naturforsch. **54a**, 272 (1999).

[7] W. P. Hong, Nuovo Cim. **B 114**, 845 (1999).

[8] Y. T. Gao and B. Tian, Int. J. Mod. Phys. **C12**, 879 (2001).

[9] B. Tian and Y. T. Gao, Z. Naturforsch., **51a**, 171 (1996).

[10] J. Weiss, M. Tabor, and G. Carnevale, J. Math. Phys. **24**, 522 (1983).

[11] B. Tian and Y. T. Gao, Phys. Lett **A 209**, 297 (1995).

[12] B. Tian and Y. T. Gao, Phys. Lett **A 212**, 247 (1996).

[13] L. N. Trefethen, Spectral Method in Matlab (Siam, 2000).

[14] Y. T. Gao and B. Tian, Computer Phys. Comm. **133**, 158 (2001).

[15] Y. T. Gao and B. Tian, Int. J. Mod. Phys. **C12**, 891 (2001).

[16] Y. T. Gao, B. Tian, and G. W. Wei, Int. J. Mod. Phys. **C12**, 1417 (2001).